CHAPTER IV
RESULTS AND DISCUSSION

4.1 Physical Appearance of the Prepared Catalysts

In this work, the catalysts for steam reforming of methanol were prepared by various methods such as incipient wetness impregnation (IWI), co-precipitation (CP), and deposition-precipitation (DP).

The loading of gold metal was defined as atomic percentage (%atom).

$$\%\ \text{atom} = \frac{\text{Au}}{\text{Au} + \text{Me}} \cdot 100\% \qquad (4.1)$$

where Au was the number of gold (atom) and Me was the number of metal (atom) that could be either cerium (Ce) or zinc (Zn) in the prepared catalyst system.

The physical properties of the prepared catalysts are shown in Table 4.1.

Table 4.1 Physical properties of the prepared gold catalysts and the supports

Catalysts	Color	Nominal gold loading(%atom)	Gold loading (%atom)*
CeO_2 (Commercial)	white	-	-
CeO_2 (Synthesis)	light yellow	-	-
ZnO (Comercial)	white	-	-
ZnO (Synthesis)	white	-	-
Au/CeO_2(5%IWI)	gray	5.00	4.82
Au/CeO_2(5%DPC)	mauve	5.00	2.92
Au/CeO_2(5%DPS)	purple	5.00	5.11
Au/CeO_2(5%CP)	dark blue	5.00	4.31
Au/CeO_2(1%CP)	light blue	1.00	0.67
Au/ZnO(5%CP)	mauve	5.00	3.90

* from ICP measurement

Galvangno *et al.*, 1978 reported that the order of particle sizes increased in the order of purple<pink<mauve for Au/Al_2O_3 catalysts. Based on their work, the different colors of catalyst might tell us roughly about the different sizes of catalyst particles.

The principle of deposition of gold catalyst on the support is the deposition of gold hydroxide on the positive surface of the support. In case of CeO_2 which have the PZC (point of zero charge) around 7.0, the gold hydroxide species can deposit on the positive charge of support surface at pH around 7.0. Therefore, pH is very important factor for catalyst preparation both co-precipitation and deposition-precipitation methods because these method necessitated gold hydroxide to deposit onto the surface of the support. In the case of SiO_2 (PZC = 1-2) support, the gold hydroxide cannot deposit on the support due to at pH which correspond to gold hydroxide form (Figure 4.1), the surface of the support already change to negative charge (above PZC) so the catalyst is inactive for the reaction (Ivanova *et al.*, 2004).

The pH of the solution and the corresponding gold chloro-hydroxy species are shown in Figure 4.1, the gold precursor ($HAuCl_4.3H_2O$) is transformed to gold hydroxide with an increase of aqueous solution pH. In this work, the pH was adjusted close to or above 7 for ensuring that the hydroxide species were available for precipitating on the support of the catalyst.

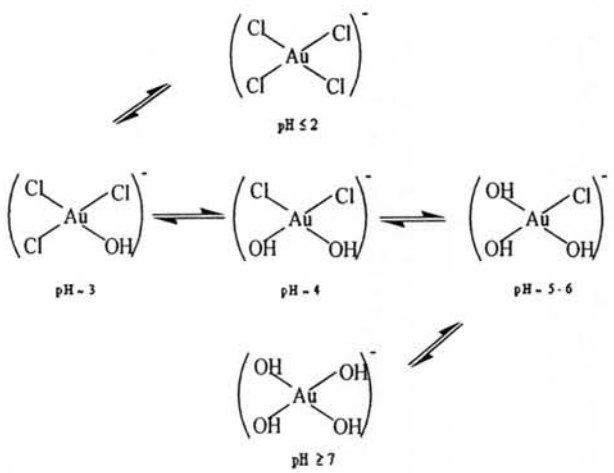

Figure 4.1 Equilibrium between gold species according to pH (Ivanova *et al.*, 2004).

The gold uptake also depended on the surface area of the support (Moreau *et al.*, 2007), there was an increase in gold uptake as the surface area of the support was raised. The idea of an equilibrium-limited adsorption of a gold precursor that there was a maximum amount of gold precursor which can deposit onto the support with particular surface area. As seen from the results of DP catalyst, the maximum of gold uptake was about 2.92% and 5.11% for commercial support and synthetic support, respectively. Hence the difference of surface area was expected as evidenced by SEM measurement.

4.2 Characteristics of the Prepared Catalysts

4.2.1 X-Ray Diffraction (XRD)

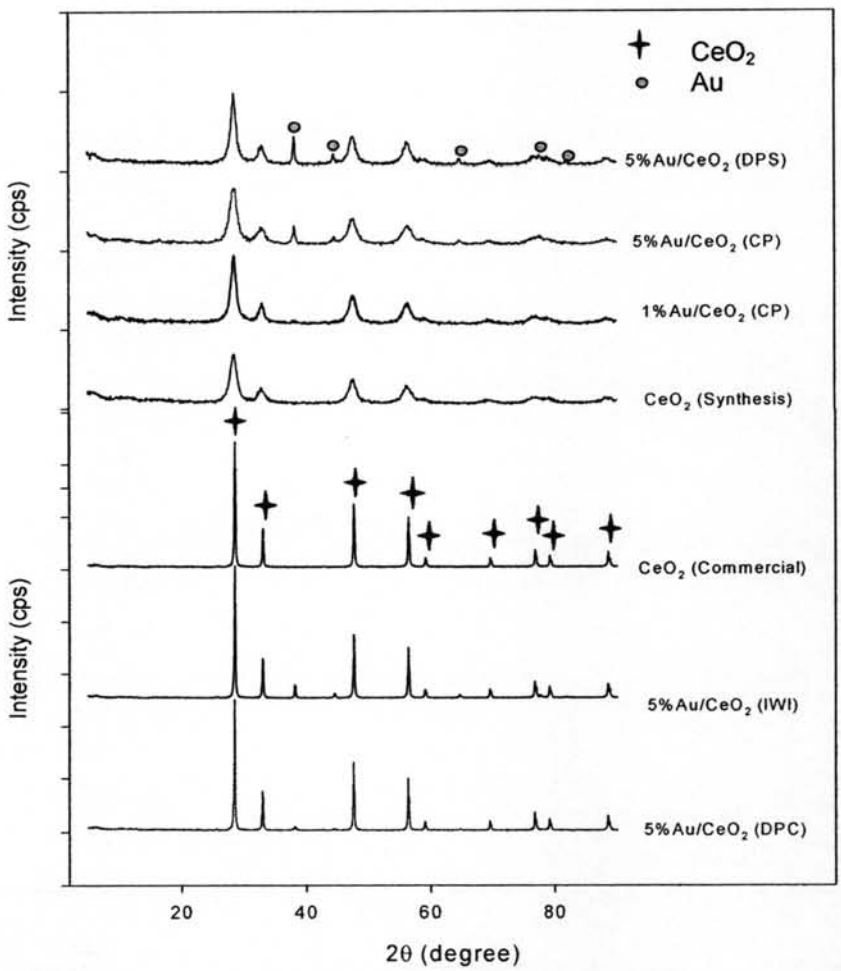

Figure 4.2 XRD patterns of the prepared gold catalysts and support.

Figure 4.2 shows the X-ray diffraction patterns of as-prepared Au/CeO_2 catalysts and CeO_2 supports. They show the presence of CeO_2 in the cubic crystal structure of fluorite type (Arena *et al.*, 2006) and the synthesis CeO_2 has lower crystallinity than commercial CeO_2 observed by the broader of XRD peak. There were some peaks corresponding to metallic gold on the surface of the catalysts. The crystallite sizes calculated by Scherrer equation are shown in Table 4.2. The CeO_2 (111) and CeO_2 (220) peaks appeared at $2\theta \approx 28.6$ and 47.5°, respectively. The diffraction peaks of Au in the XRD patterns at $2\theta \approx 38.2$, 44.4, 64.7, 77.6, and 81.9° were observed in the spectra corresponding to Au (111), Au (200), Au (220), Au (311), and Au (222), respectively.

Table 4.2 Crystallite sizes of the prepared Au/CeO_2 catalysts and CeO_2 support

Catlysts	Ce (111)	Ce (220)	Au (111)	Au (200)	Au (220)	Au (311)	Au (222)
CeO_2 (Syn.)	6.05	5.62					
CeO_2 (Com.)	37.32	33.75					
Au/CeO_2(1%CP)	8.14	6.39	15.47				
Au/CeO_2(5%CP)	5.73	5.18	21.64	17.74	13.77	3.83	36.92
Au/CeO_2(5%DPS)	8.20	6.94	25.14	20.69	4.12	7.59	15.81
Au/CeO_2(5%DPC)	40.38	36.33	32.78	31.25	20.19	28.44	
Au/CeO_2(5%IWI)	40.31	35.46	39.95	34.02	28.98	29.53	35.41

* crystallite size in nm

It was found that the synthesis ceria had a smaller crystallite size than the commercial ceria and when gold was loaded onto the ceria (Figure 4.3 (a)), the crystallite size of ceria trended to increase due to the interaction between gold and cerium atom. The crystallite size of Ce (111) at $2\theta \approx 28.6^{\circ}$ and Ce (220) at $2\theta \approx 47.5^{\circ}$ increased in the order of Au/CeO_2(5%CP)< Synthesis CeO_2< Au/CeO_2(1%CP)< Au/CeO_2(DPS)< Commercial CeO_2< Au/CeO_2(IWI)< Au/CeO_2(DPC), respectively.

Moreover, it was also observed that there are 2 trends of gold crystallite size as shown in the Figure 4.3 (b) and (c). For Au (111), Au (200), and Au (311), the

gold crystallite size increased in the order of Au/CeO_2(1%CP)< Au/CeO_2(5%CP)< Au/CeO_2(DPS)< Au/CeO_2(DPC)< Au/CeO_2(IWI), respectively. Another trend was observed for Au (220) and Au (222) that DPS catalyst showed the minimum in Au crystallite size (Figure 4.3 (c)).

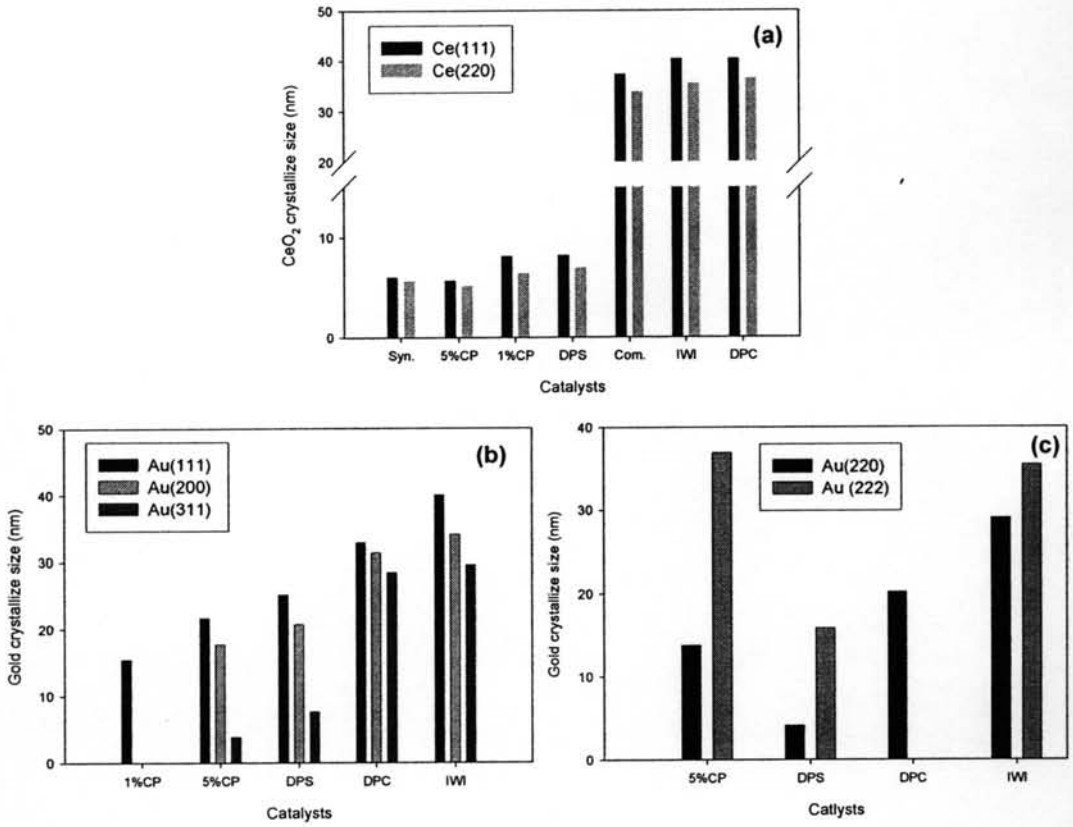

Figure 4.3 Ceria and gold crystallite sizes of the prepared catalysts: (a) Ceria crystallite size, (b) Au (111), Au (200), and Au (311) crystallite size, (c) Au (220) and Au (222) crystallite size.

Haruta and Daté (2001) illustrated the dependency of gold particle size on chemical reactions such as epoxidation of propylene, water-gas-shift reaction, hydrogenation of unsaturated hydrocarbons, and liquid-phase selective oxidation. Au/TiO_2 was active for CO oxidation at 350 K (77 °C), turn over frequency (TOF) for CO oxidation reaches a maximum at a diameter of Au islands of 3.5 nm where Au partially loosed its metallic nature. Au/TiO_2 used epoxidation to propylene produce pro-

pylene oxide and the results showed that as a gold particles larger than 2.0 nm in diameter produce propylene oxide, whereas smaller gold particles produce propane (Hayashi *et al.*, 1998). The acetylene hydrogenation over Au/Al_2O_3 (Jia *et al.*, 2000), catalyst reached maximum at gold particles size of about 3.0 nm in diameter, eventually the catalytic activity dropped as the gold particle size further decreased.

For steam reforming of methanol over supported gold catalyst, there was diminutive information about the relationship between gold particle size and the catalytic activity so this work facilitated to understand the dependence of gold particle on catalytic activity in SRM.

4.2.2 Scanning Electron Microscopy (SEM)

The morphology of the catalysts was studied by Scanning Electron Microscopy (SEM) as shown in the Figure 4.4.

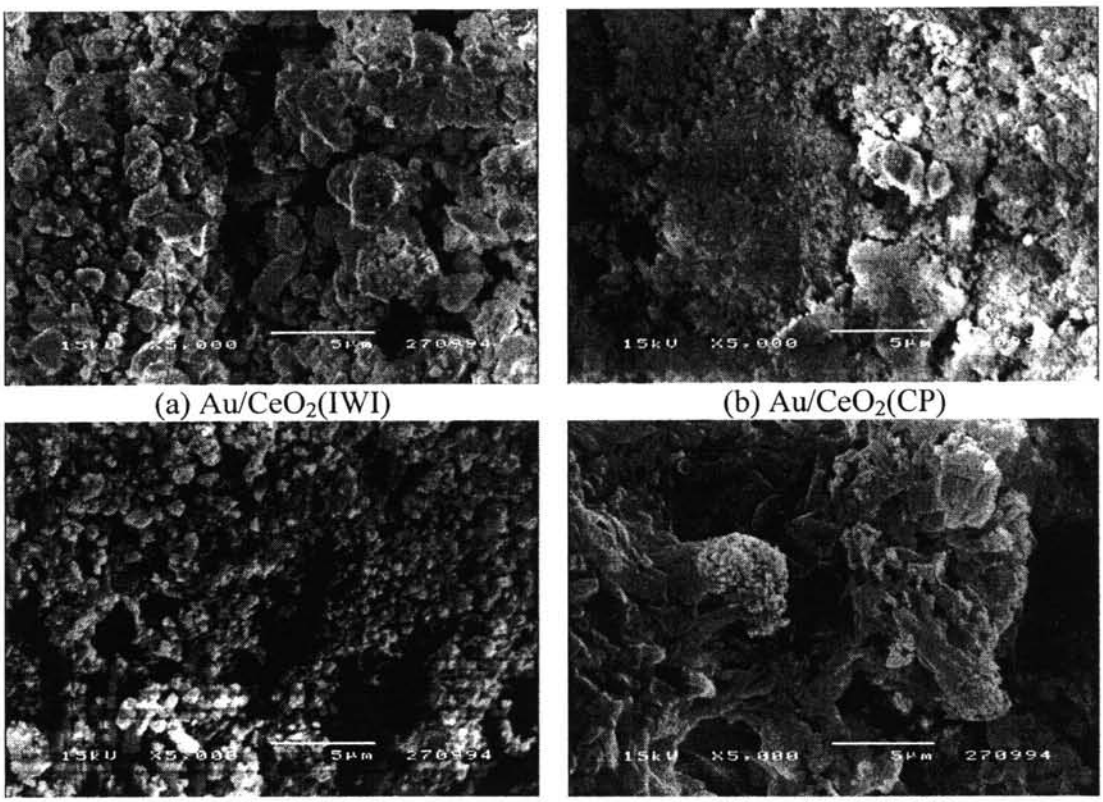

(a) Au/CeO_2(IWI) (b) Au/CeO_2(CP)

(c) Au/CeO_2(DPC) (d) Au/CeO_2(DPS)

Figure 4.4 The morphology of prepared catalysts: (a) Au/CeO_2(IWI), (b) Au/CeO_2(CP), (c) Au/CeO_2(DPC), and (d) Au/CeO_2(DPS)

The difference morphology of the prepared catalysts was clearly observed. The incipient wetness impregnation and deposition precipitation method provided the small particle on the surface of the catalyst while the co-precipitation provided the small flake of ceria particle.

4.2.3 Transmission Electron Microscopy (TEM)

The structure of gold particle on ceria did not show clear small gold clusters on ceria by Transmission Electron Microscopy (TEM) caused by the disturbance of the diffraction and phase contrast by ceria (Akita *et al.*, 2006).

The TEM images the catalysts are shown in Figure 4.5. This Figure revealed several notices. The larger of ceria crystallite size (from XRD) the clearer of TEM image in distinguishing ceria and gold particle. It seem that larger ceria crystallite size (commercial ceria) gave the differentiable TEM image of gold and ceria particle while for the smaller ceria crystallite size (synthesis ceria), it hardly to identify the gold and ceria particle. It seem that when synthesis ceria is used the gold was well dispersed in the support so we can see the homogeneous texture of catalyst (Figure 4.5 (b), (d), and (e)). The deposition-precipitate catalyst (Figure 4.5 (c)), the gold particle, small round shape and lighter color, deposited onto the outer surface of the catalyst as expected. For the distinguishable catalyst (DPC and IWI), the comparison of gold particle size from XRD and TEM was summarized in Table 4.3.

Table 4.3 Comparison of gold particle size form XRD and TEM analysis

Catlysts	Au (111) (nm)*	Au (220) (nm)*	gold particle size (nm)+
Au/CeO_2(5%DPC)	32.78	20.19	22.85 ± 1.56
Au/CeO_2(5%IWI)	39.95	28.98	20.65 ± 6.27

*from XRD, +from TEM

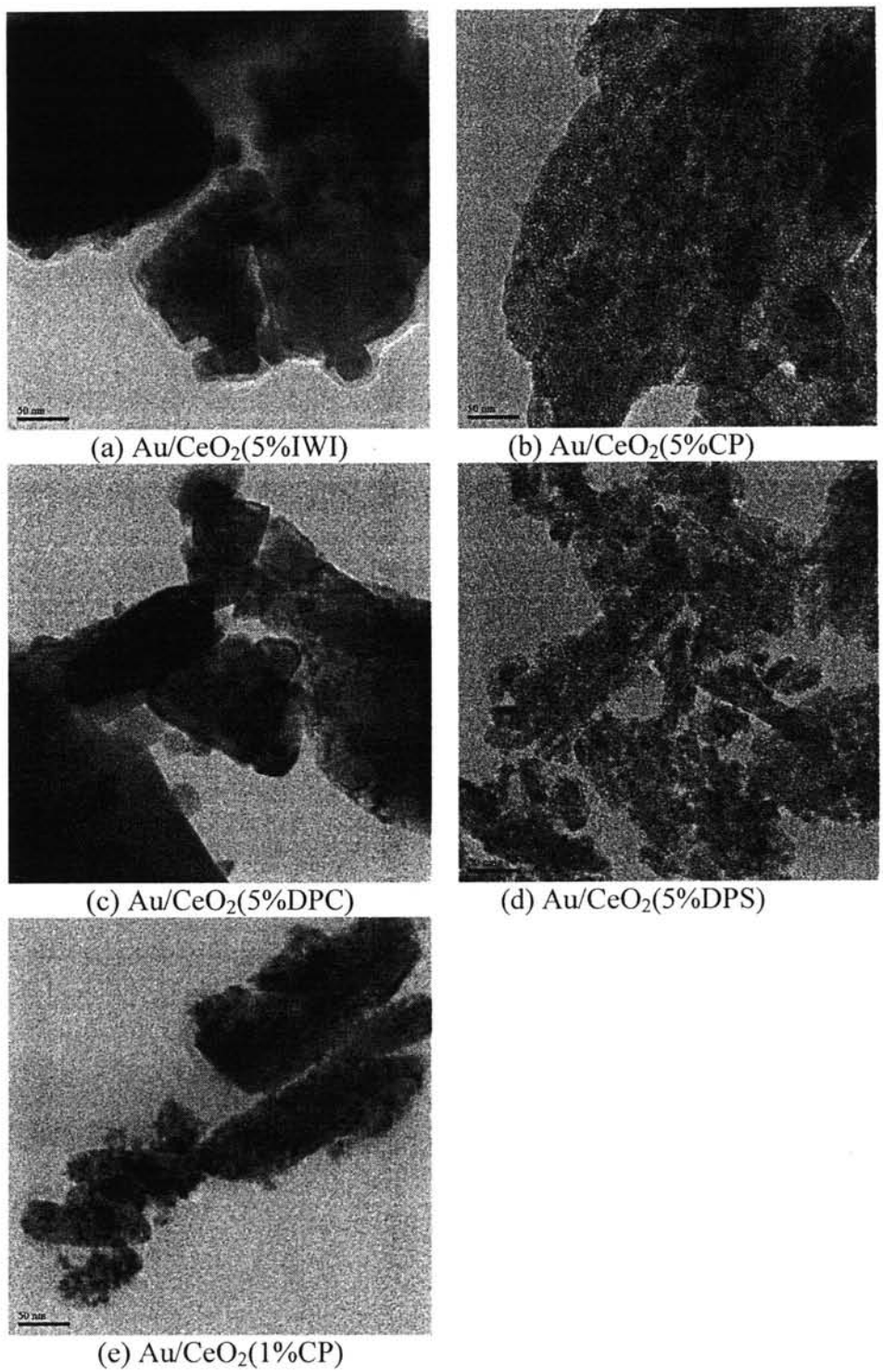

(a) Au/CeO_2(5%IWI) (b) Au/CeO_2(5%CP)

(c) Au/CeO_2(5%DPC) (d) Au/CeO_2(5%DPS)

(e) Au/CeO_2(1%CP)

Figure 4.5 TEM images of the prepared catalysts: (a) Au/CeO_2(5%IWI), (b) Au/CeO_2(5%CP), (c) Au/CeO_2(5%DPC), (d) Au/CeO_2(5%DPS), and (e). Au/CeO_2(1%CP).

The particle size from TEM analysis was close to the value of Au (220) crystallite size that was the second type gold crystallite size trend as described above in section 4.2.1.

4.2.4 Temperature Programmed Reduction (TPR)

The H_2-TPR technique is used to study the surface and bulk oxygen reducibility of ceria supported catalysts. The H_2-TPR profile of ceria contains two major peaks, one at lower temperature (~500°C) attributed to the reduction of surface oxygen species and the other one at high temperatures (above 800°C) attributed to the reduction of bulk oxygen and the formation of the lower oxides of cerium (Arena *et al.*, 2006).

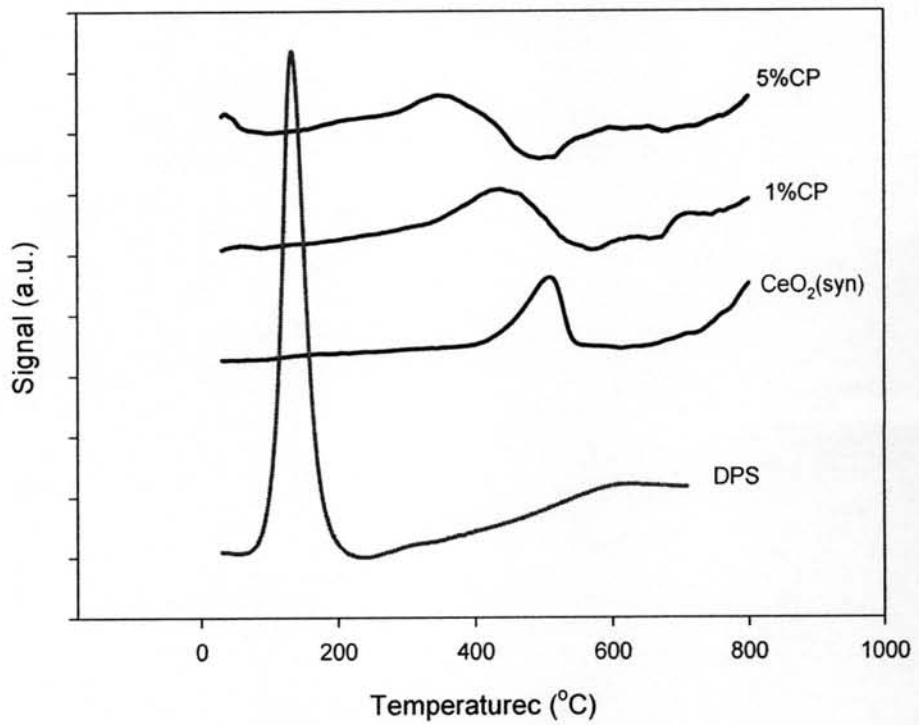

Figure 4.6 TPR profiles of the prepared supported Au catalysts and CeO_2 supports.

It was observed that the presence of gold causes the strongly effect on the reducibility of the ceria. The first peak was shifted significantly to lower tem-

perature in the presence of gold; therefore, gold can enhance the reduction behavior of the ceria.

The DPS catalyst is the easiest reducibility evidenced by the lowest reduction temperature (~210°C) and lowest area under TPR profile. The order of reduction increases in the order of 5%DPS < 5%CP < 1%CP, respectively.

The different catalyst preparation provides the different catalyst characteristics such as physical appearance, gold and ceria particle size, morphology, and reduction temperature. We demonstrated how dissimilar of each catalyst in catalytic activity in the next section.

4.3 Activity Measurement

Catalytic activity studies were conducted in a pyrex glass cylinder tube having an internal diameter of 6.0 mm at reaction temperature range of 200 - 450°C and atmospheric pressure. One hundred mg of catalyst was used. The reactant contained liquid methanol and water with the molar ratio of water to methanol equal 1.33. When the reactant formed a vapor, it was carried by helium (50% by volume of the feed to reactor) through the reactor tube.

4.3.1 Effect of Catalyst Pretreatment

For Au/CeO_2 (CP), the reaction condition was carried at 400°C at a steam to methanol molar ratio of 1.33, 0.1g catalyst, 1.5 mL/hr of liquid flowrate and 34 mL/min of carrier gas (He).

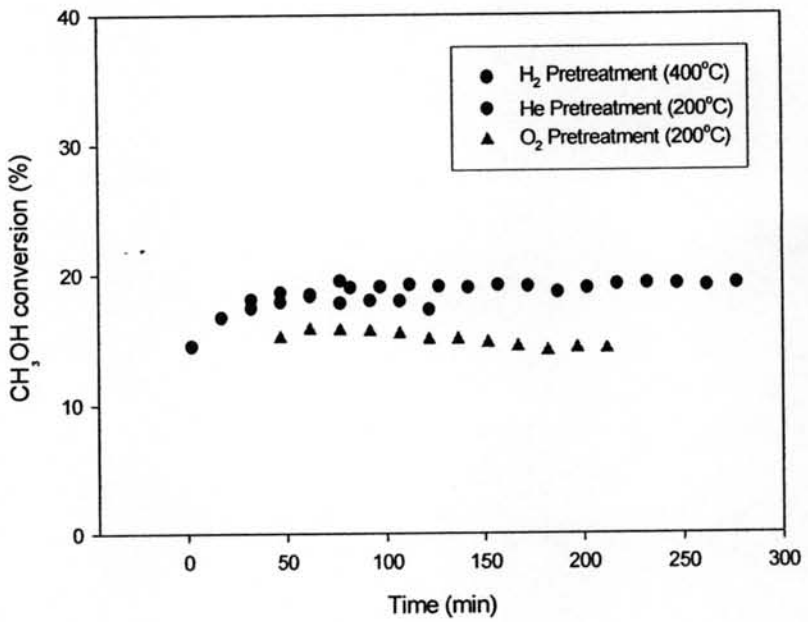

Figure 4.7 Effect of the catalyst pretreatment on methanol conversion.

The pretreatment of catalyst prior to the reaction is very important for chemical reaction. The different pretreatment will provide different state of gold catalyst. It is of interest to investigate the effect of pretreatments, H_2, He, and O_2, on

the Au/CeO_2 catalyst and subsequent their catalytic activity. It will be gold metallic for H_2 pretreatment and it will be gold oxide for O_2 pretreatment. It was found that the activity of the catalysts in term of CH_3OH conversion is not much differnce when comparing with H_2 and He pretreatment. It is not surprise because we have H_2 in the product stream and the catalyst will automatically reduced by H_2 therefore it is not different for H_2 and He pretreatment. But the conversion is slightly lower for O_2 pre-treatment. For those results it can conclude that the SRM prefer metallic gold rather than gold oxide form of the catalyst.

For the selectivity, all 3 pretreatment conditions did not give different in H_2, CO_2 and CO selectivity.

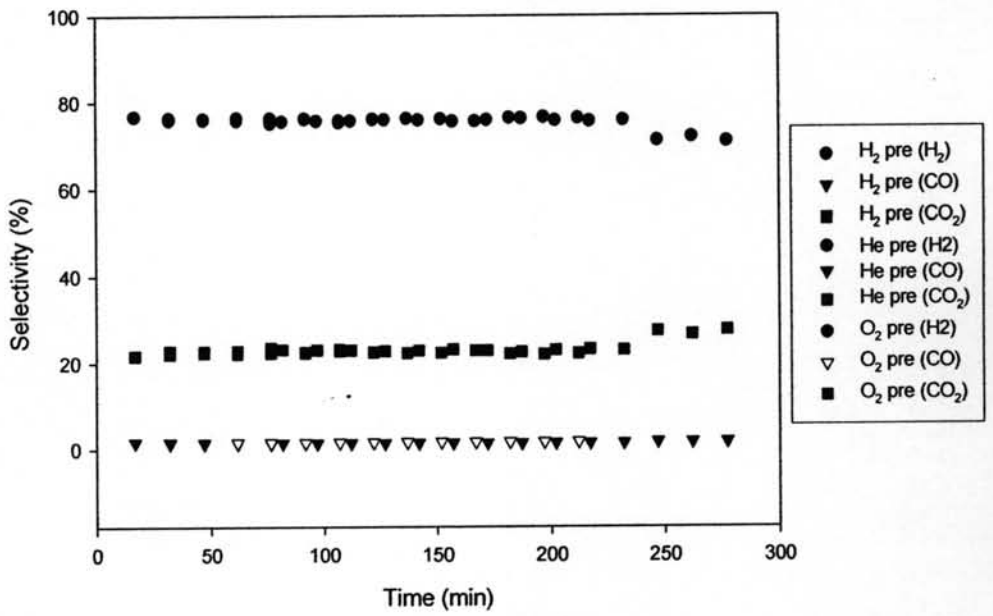

Figure 4.8 Effect of the catalyst pretreatment on product selectivity.

For the CO/CO_2 ratio, the H_2 pretreatment gave the lowest amount of this ratio. Typically, fuel cell application prefers a small amount of CO for a good performance of fuel cells stack. For the next study, H_2 pretreatment was selected because high CH_3OH conversion and less amount of CO were obtained.

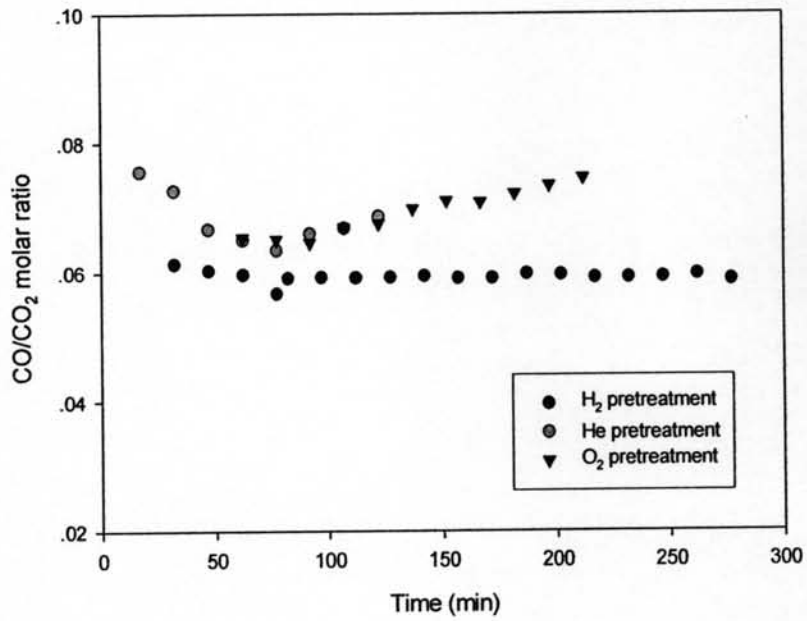

Figure 4.9 Effect of the catalyst pretreatment on CO/CO_2 on the product stream.

4.3.2 Effect of Catalyst Preparation and Reaction Temperature

Among the catalyst listed, the Au/CeO_2(DPS) showed the best performance in hydrogen production by steam reforming of methanol. It gave the maximum CH_3OH conversion of > 80% which is lower than the maximum conversion reported in the literature (copper based catalyts).

Table 4.4 The catalytic performance of Au/CeO_2 catalysts in SRM

Catalyst	Reaction Temp. (oC)	MeOH conversion Mol.%	H_2 prod. mmol/hr	CO/CO_2	Products distribution Mol. %			
					H_2	CO	CH_4	CO_2
DPC	300	0.05	-	0	-	-	-	100
	350	0.08	-	0	-	-	-	100
	400	0.55	0.855	0.06	86.77	0.75	-	12.49
	450	2.22	2.285	0.08	81.44	1.43	-	17.13
IWI	300	0.16	-	0	-	-	-	100
	400	3.74	2.880	0.63	76.60	9.03	-	14.36
	450	15.41	8.902	1.12	71.04	15.01	0.55	13.40
1%CP	240	0.24	-	0	-	-	-	100
	280	0.24	-	0.39	-	28.05	-	71.95
	300	0.28	-	0.39	-	28.25	-	71.75
	350	1.01	1.098	1.34	82.33	10.12	-	7.55
	400	5.10	3.280	2.49	73.23	17.88	1.71	7.18
	450	21.25	9.401	3.19	65.37	20.85	7.27	6.52
5%CP	260	0.21	-	0	-	-	-	100
	280	0.42	-	0	-	-	-	100
	300	0.93	1.053	0	82.88	-	-	17.12
	350	4.67	3.729	0.03	77.26	0.71	-	22.03
	400	17.16	11.924	0.06	74.73	1.45	-	23.82
	450	45.94	30.910	0.12	74.11	2.71	0.24	22.94
DPS	200	0.18	-	0	-	-	-	100
	250	0.45	-	0	-	-	-	100
	300	2.35	2.332	0	80.88	-	-	19.12
	350	11.89	8.852	0.03	76.02	0.62	-	23.36
	400	61.51	43.993	0.04	75.27	0.98	-	23.75
	450	84.24	59.108	0.14	74.91	3.08	0.06	21.95

Table 4.4 summaries the catalytic performance and product distribution of Au/CeO_2 catalysts in steam reforming of methanol with various conditions. The reaction was carried out at steam to methanol molar ratio of 1.33, 0.1g catalyst, 1.5 mL/hr of liquid flowrate and 34 mL/min of carrier gas (He).

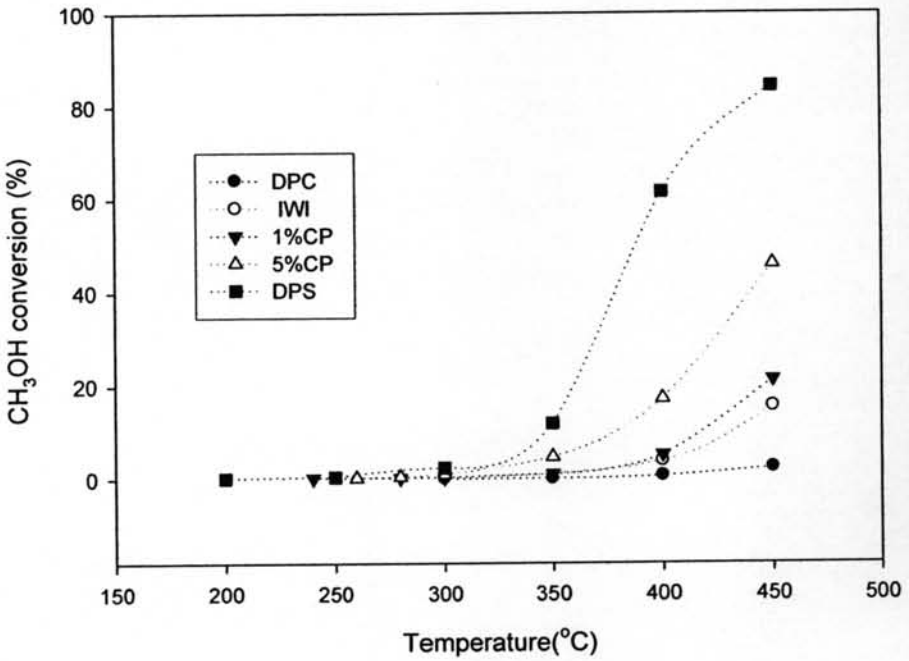

Figure 4.10 Effect of reaction temperature on methanol conversion.

The higher reaction temperature, the higher CH_3OH conversion was observed and the Au/CeO_2(DPS) showed the best performance in hydrogen production by steam reforming of methanol.

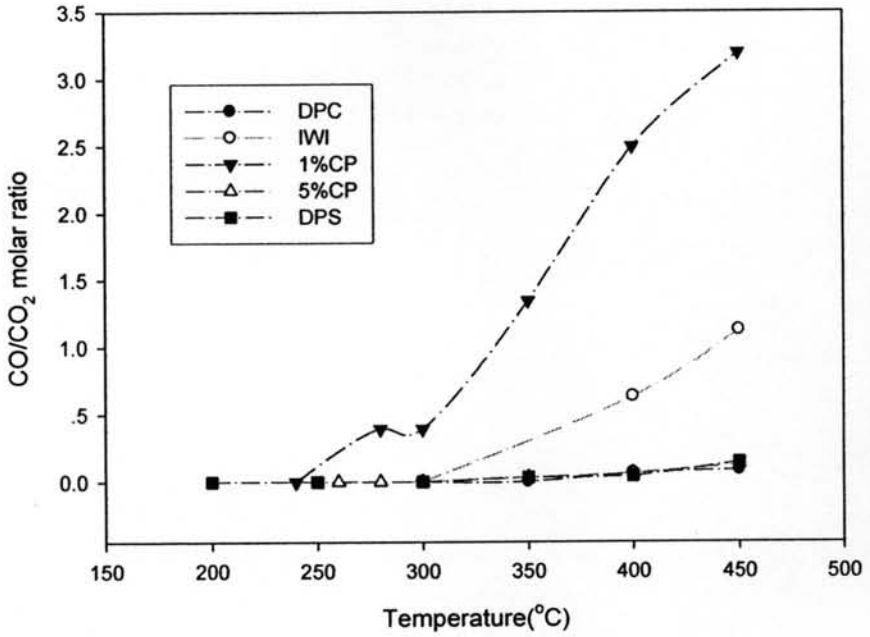

Figure 4.11 CO/CO_2 molar ratios versus reaction temperature.

Figure 4.11 shows the CO/CO_2 molar ratio, when increasing temperature this ratio trend to decrease that because more CO was produced by methanol decomposition reaction.

A comparison of the effect of catalyst preparation on CO/CO_2 molar ratio over Au/CeO_2 catalyst is presented in Figure 4.11. The results indicated that the catalyst preparation showed a significant effect, the CO/CO_2 molar ration increased in order of DPC≈DPS≈5%CP<IWI<1%CP, respectively. The IWI and 1%CP methods were not suitable for using in hydrogen production that requires a trace amount of CO content for fuel cell applications. From CO/CO_2 ratio results, IWI and 1%CP catalysts gave quite high CO/CO_2 ratio compared to other methods, hence, this method was not recommended for fuel cell applications.

By considering the formation of CH_4, it might be formed through reaction (4.2) because the available of heat source at high temperature and the reactants (CO and H_2).

$$CO_{(g)} + 3H_{2(g)} \leftrightarrow CH_{4\,(g)} + H_2O_{(g)} \quad \Delta H^0 = -206.4\ kJ/mol \qquad (4.2)$$

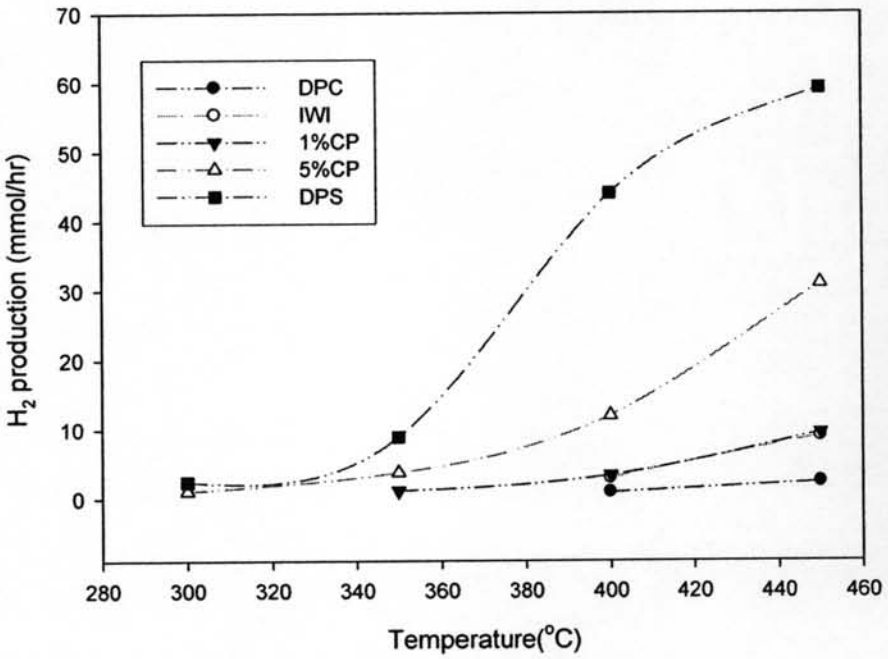

Figure 4.12 Effect of reaction temperature on H_2 production.

Figure 4.12 shows the H_2 production versus temperature. The increasing of reaction temperature, H_2 production rate trended to increase because of more energy that can supply to the reaction.

4.3.2.1 Size dependency in the SRM of gold catalysts

The effect of crystallite size of gold on the steam reforming of methanol and decomposition of methanol was discussed in this section.

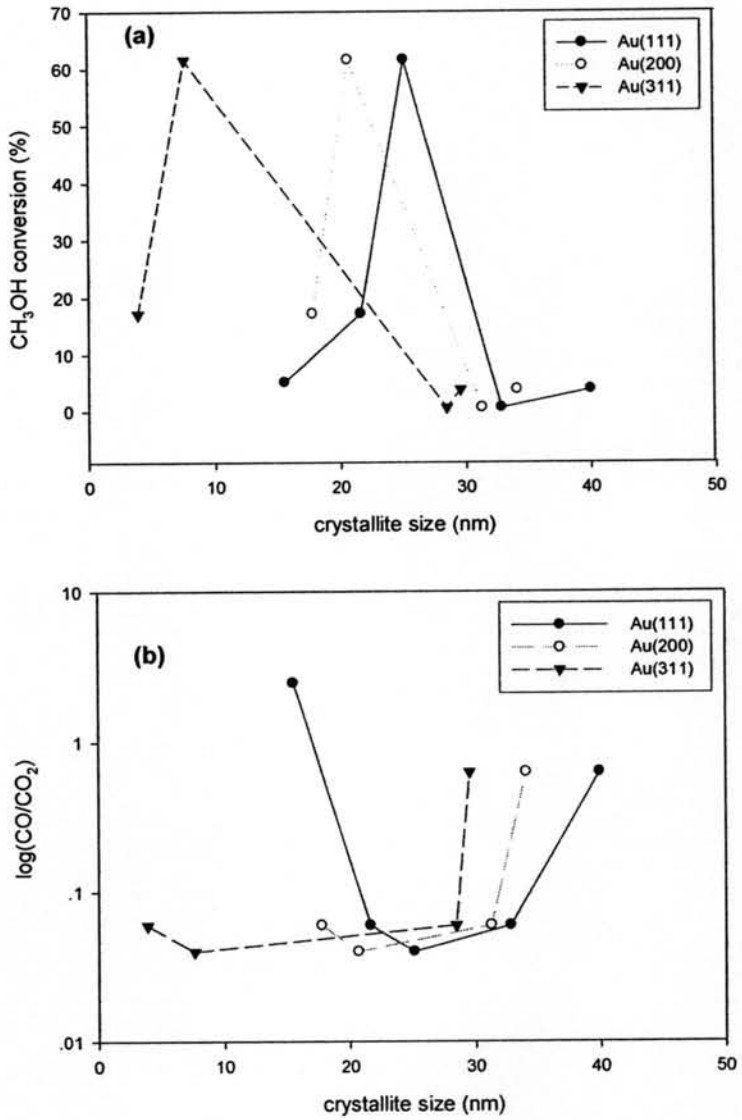

Figure 4.13 gold crystallite size versus methanol conversion (a) and CO/CO_2 (b) of Au(111), Au(331), and Au(200) in SRM reaction.

All 3 planes of metallic gold ((111), (200), and (311)) showed the same tendency of methanol conversion and CO/CO_2 molar ratio as illus-

trated in Figure 4.13. the crystallite size of gold increase in the order of 1%CP < 5% CP < DPS < DPC < IWI, respectively. The highest methanol conversion and lowest CO/CO_2 achieved at moderate gold crystallite size (DPS catalyst).

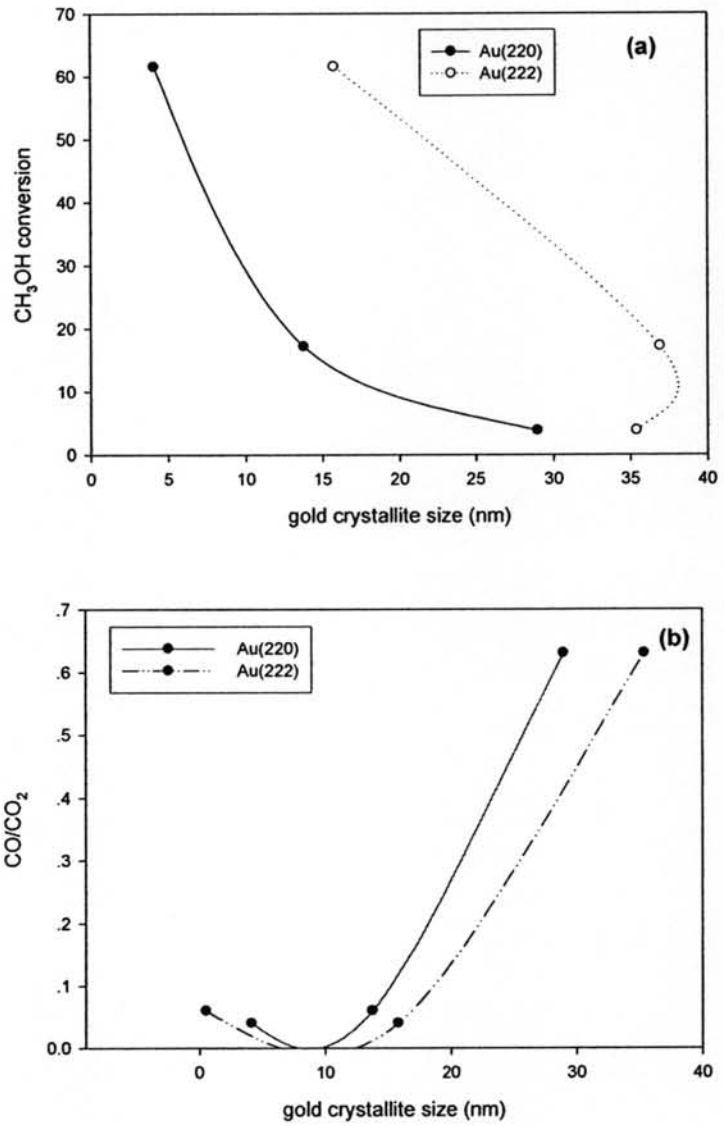

Figure 4.14 gold crystallite size versus methanol conversion (a) and CO/CO_2 (b) of Au(220) and Au(222) planes.in SRM reaction.

For Au(220) and Au(222) which also showed the similar tendency in gold crystallite size. The crystallite size was in the order of

DPS<DPC<5%CP < IWI for Au(220) but for Au(222), DPC had the smallest gold crystallite size.

The maximum methanol conversion and very low CO/CO_2 accomplished from DPS catalyst which had smallest of gold crystallite size of Au(220).

4.3.3 Effect of steam to methanol (s/m) molar ratio

4.3.3.1 Decomposition of methanol (DM)

Decomposition of methanol (4.3) is the one candidate reaction for onboard hydrogen production in fuel cell applications.

$$CH_3OH_{(g)} \leftrightarrow H_{2\,(g)} + CO_{(g)} \quad \Delta H^0 = 91 \text{ kJ/mol} \qquad (4.3)$$

The decomposition of methanol reaction was performed over gold supported catalysts prepared by various catalyst preparations. The reaction conditions were 1.5 mL/hr of liquid flowrate and 34 mL/min of carrier gas (He) and temperature range of 250 - 450°C .

Table 4.5 The catalytic performance of gold catalysts in DM

Catalyst	Reaction Temp. (°C)	MeOH conversion Mol.%	H_2 prod. mMol/hr	CO/CO_2	Products distribution Mol. %			
					H_2	CO	CH_4	CO_2
DPC	400	0.31	0.917	0.33	88.72	2.82	-	8.46
	450	0.77	1.350	2.64	82.40	10.00	3.67	3.93
IWI	350	0.09	-	∞	-	100.00	-	-
	400	0.69	0.955	4.92	78.89	17.46	0.00	3.65
	450	3.29	3.022	22.71	71.17	23.98	3.80	1.06
1%CP	250	0.02	-	∞	-	100	-	-
	300	0.19	-	∞	-	100	-	-
	350	1.49	2.034	∞	78.62	21.38	0.00	0.00
	400	6.97	5.983	41.86	69.78	26.34	3.26	0.63
	450	24.87	15.489	15.14	62.60	26.16	9.50	1.73
5%CP	250	0.08	-	0.00	-	-	-	100
	300	0.46	0.986	0.12	85.16	1.59	0.00	13.25
	350	2.24	3.262	0.41	79.68	5.93	0.00	14.38
	400	8.59	8.945	1.82	73.68	16.46	0.79	9.07
	450	21.04	17.879	2.98	69.55	20.14	3.56	6.75
DPS	250	0.21	-	0.00	-	-	-	100
	300	1.44	2.305	0.20	80.90	3.20	-	15.9
	350	4.24	4.681	1.36	74.79	13.64	1.54	10.04
	400	12.83	12.833	1.99	72.81	16.97	1.68	8.53
	450	25.53	24.034	3.68	71.66	21.43	1.09	5.82
Zn	250	0.15	-	0.00	-	-	-	100
	300	1.59	2.419	3.45	80.33	15.25	0.00	4.42
	350	14.10	13.034	10.71	71.31	25.00	1.35	2.33
	400	26.43	23.112	6.19	70.16	23.60	2.42	3.83
	450	26.59	22.444	3.95	69.66	21.75	3.48	5.10

Even though theoretically, the decomposition of methanol should produce only CO and H_2 a products but others products were detected such as CO_2 and CH_4 that were produced via DM reaction. The observed results in products distribution might correspond to the mechanism that proposed by Choi *et al.* (2002) which methanol can decompose to from an intermediate and decomposed further to from CO_2 or CO. The formation of CH_4 at high temperature might from via reaction (4.2) as the same reasons for steam reforming of methanol.

4.3.3.2 Effect of steam to methanol (s/m) molar ratio

A comparison of methanol conversion with different steam to methanol molar ratio is illustrated for 5%CP and DPS catalysts as shown in Figure 4.14. In this work, it was revealed that when increasing s/m, ratio the methanol conversion trend to increase but it reached the maximum conversion (~45 – 80%) at s/m = 1.33 compared to s/m = 2.

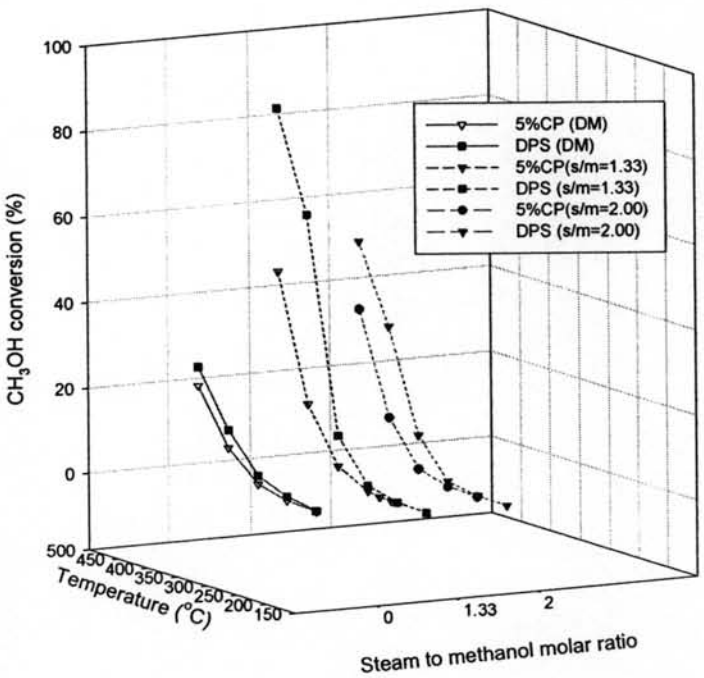

Figure 4.15 Effect s/m molar ratio on methanol conversion

The presence of steam in the feed helps to decrease unwanted products like CH_4 and CO. Typically, the steam to methanol molar ratio was used in the range of 1.00 – 2.00 for steam reforming of methanol. Even though, increasing of s/m molar ration trended to decrease CO content but it reached the minimum CO content around s/m = 1.40 (Patel and Pant *et al.*, 2006).

Table 4.6 The catalytic performance of gold catalysts in SRM with s/m=2.00

Catalyst	Reaction Temp. (oC)	MeOH conversion Mol.%	H_2 prod. mMol/hr	CO/CO_2	Products distribution Mol. %			
					H_2	CO	CH_4	CO_2
5%CP	250	0.08	-	0	-	-	-	100
	300	0.35	-	0	-	-	-	100
	350	2.42	2.128	0.08	81.84	1.43	-	16.73
	400	12.30	7.826	0.15	76.50	3.07	-	20.43
	450	35.61	21.096	0.23	75.14	4.66	0.39	19.82
1%CP	250	0.08	-	0	-	-	-	100
	300	0.32	-	0.57	-	36.75	-	63.25
	350	2.17	1.685	1.30	79.82	11.40	-	8.78
	400	9.68	5.373	2.12	73.90	17.25	0.73	8.12
	450	27.34	12.464	2.66	69.93	19.70	2.94	7.42
5%DPS	200	0.08	-	0	-	-	-	100
	250	0.24	-	0	-	-	-	100
	300	1.57	1.419	0.02	82.23	0.27	-	17.51
	350	10.23	6.610	0.03	76.73	0.72	-	22.55
	400	33.56	20.985	0.05	76.13	2.44	0.08	21.40
	450	51.31	31.890	0.12	76.05	2.52	0.08	21.36
Au/ZnO	200	0.13	-	-	-	-	-	100
	250	0.57	0.988	-	89.85	-	-	10.15
	300	3.89	3.083	-	80.18	-	-	19.82
	350	17.60	11.157	0.007	76.39	0.16	-	23.45
	400	59.22	37.778	0.015	76.49	0.76	-	23.05
	450	79.85	50.598	0.031	76.38	0.71	-	22.91

4.3.4 Effect of catalyst support

Au/ZnO was introduced for studying the effect of catalyst support based on the copper-based catalyst that using ZnO as a catalyst support. In case of copper-based catalyst, the complete conversion of methanol can be achieved at the reaction temperature around 300°C but this type of catalyst had a problem that mentioned earlier.

4.3.4.1 Properties of Au/ZnO

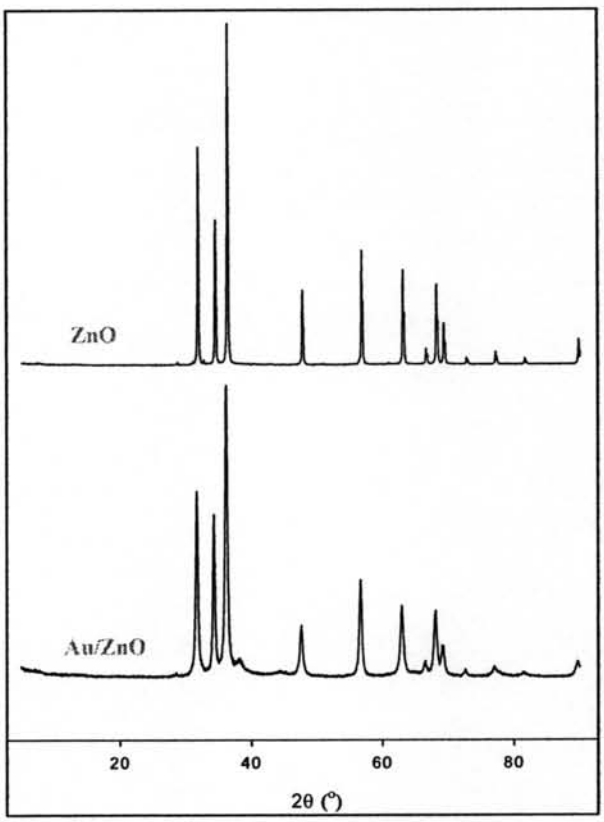

Figure 4.16 XRD patterns of the prepared Au/ZnO catalysts and support.

Au/ZnO was prepared by co-precipitation method with 5% at but it was observed by ICP that gold loading is 3.90%at. Figure 4.15 shows XRD pattern of prepared Au/ZnO catalyst. It reveals that Au (111), Au (200), and Au (220) crystallite size are 5.22, 3.50, and 5.11, respectively. This gold crystallite sizes are agree with the result from TEM analysis as shows in Figure 4.15. Au particle size is about 4.40 ± 1.05 nm.

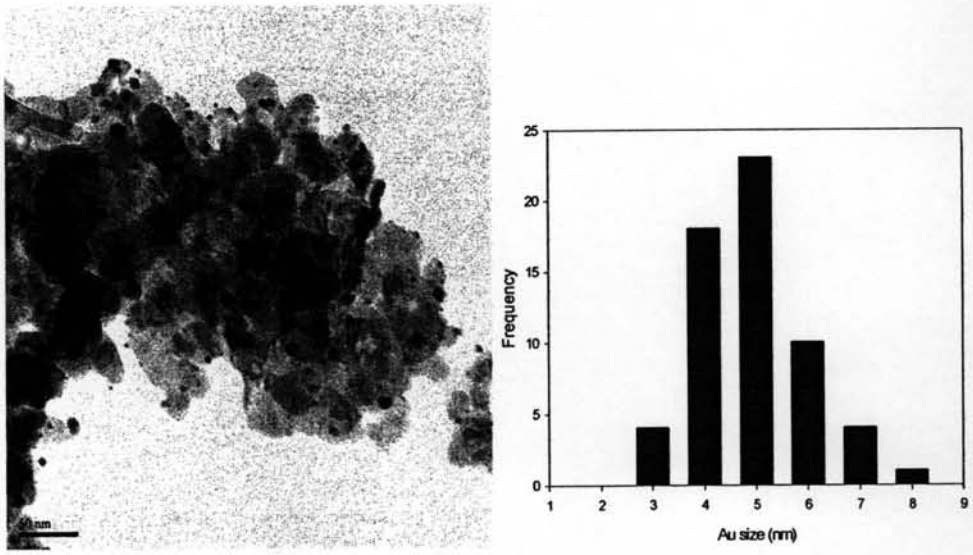

Figure 4.17 TEM analysis of Au/ZnO.

The observed gold crystallite size of Au/ZnO is less than Au/CeO_2 for almost cases except for Au (220) which the smallest Au/CeO_2 (DPS) is about 4.12 nm.

4.3.4.2 Catalytic activity of Au/ZnO

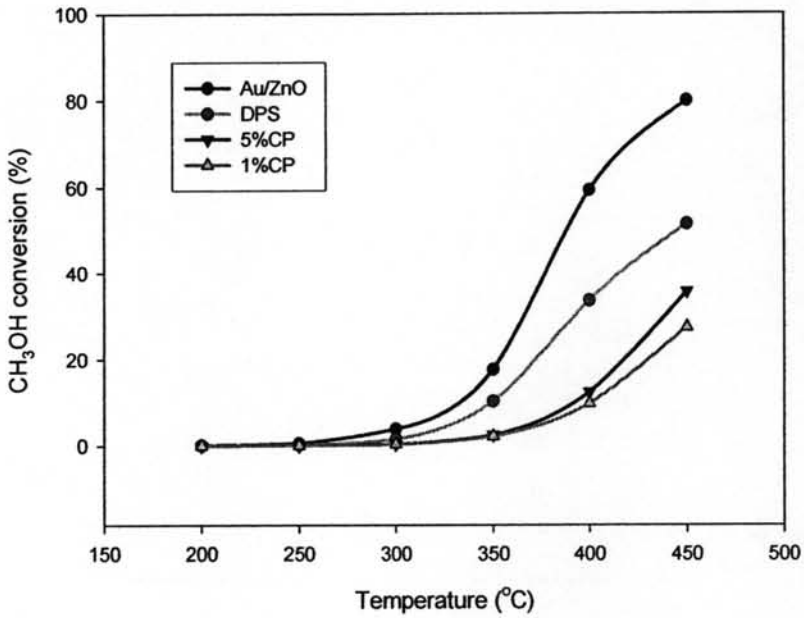

Figure 4.18 Comparison of catalytic activity Au/CeO_2 and Au/ZnO.

Figure 4.17 shows the comparison of Au/CeO_2 and Au/ZnO that tests at the reaction condition was carried at 200 - 450°C at a steam to methanol molar ratio of 2.00, 0.1g catalyst, 1.5 mL/hr of liquid flowrate and 34 mL/min of carrier gas (He).

Au/ZnO gives better in methanol conversion. From the Au (220) crystallite size

4.3.5 Stability Test

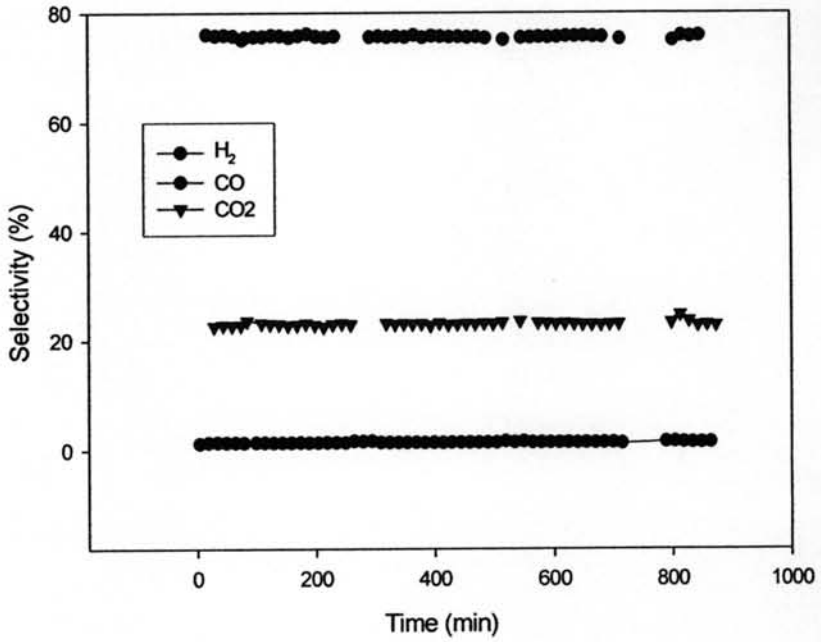

Figure 4.19 Stability of Au/CeO_2 catalysts in SRM.

The long time stability of the prepared catalysts was studied for methanol steam forming for about 15 hours as shown in Figure 4.18. The study was conducted at a steam/methanol molar ratio of 1.33, and the catalysts was Au/CeO_2(CP). The reaction conditions were kept constant at temperature of 400°C. The stability of the catalyst in term of product selectivity is illustrated in Figure 4.18. It was found that within stability test period, all catalysts showed good performance.

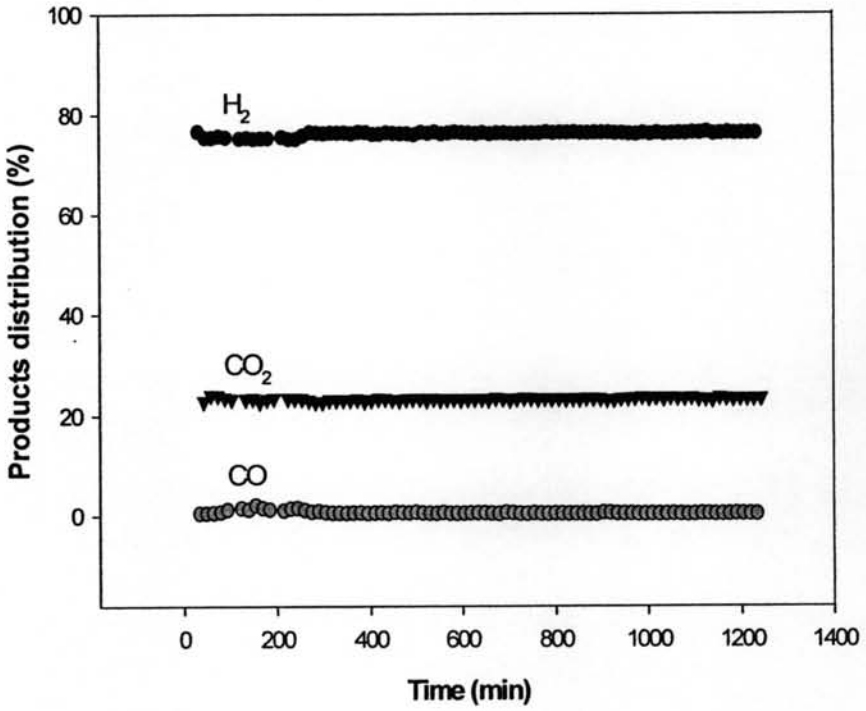

Figure 4.20 Stability of Au/ZnO catalysts in SRM.

Au/ZnO was also test for long term stability. The study was conducted at a steam/methanol molar ratio of 1.33 The reaction conditions were kept constant at temperature of 400°C.

The preliminary result showed that the gold catalyst seems to be a good catalyst for hydrogen production via steam reforming of methanol which can be operated at lower temperature comparing with the reforming of methane or ethanol. The steam reforming of methanol is the promising candidate for hydrogen production in fuel cell applications.